Global Change Biology

Global Change Biology (2017) **23**, 906–919, doi: 10.1111/gcb.13463

Ecosystem fluxes of hydrogen in a mid-latitude forest driven by soil microorganisms and plants

LAURA K. MEREDITH[1,2], RÓISÍN COMMANE[3], TREVOR F. KEENAN[4], STEPHEN T. KLOSTERMAN[5], J. WILLIAM MUNGER[3], PAMELA H. TEMPLER[6], JIANWU TANG[7], STEVEN C. WOFSY[3] and RONALD G. PRINN[2]

[1]*Department of Ecology and Evolutionary Biology, University of Arizona, Tucson, AZ, USA,* [2]*Department of Earth, Atmospheric and Planetary Science, Massachusetts Institute of Technology, Cambridge, MA, USA,* [3]*Department of Earth and Planetary Science, School of Engineering and Applied Sciences, Harvard University, Cambridge, MA, USA,* [4]*Earth Sciences Division, Lawrence Berkeley National Laboratory, Berkeley, CA, USA,* [5]*Department of Organismic and Evolutionary Biology, Harvard University, Cambridge, MA, USA,* [6]*Department of Biology, Boston University, Boston, MA, USA,* [7]*Ecosystems Center, Marine Biological Laboratory, Woods Hole, MA, USA*

Abstract

Molecular hydrogen (H_2) is an atmospheric trace gas with a large microbe-mediated soil sink, yet cycling of this compound throughout ecosystems is poorly understood. Measurements of the sources and sinks of H_2 in various ecosystems are sparse, resulting in large uncertainties in the global H_2 budget. Constraining the H_2 cycle is critical to understanding its role in atmospheric chemistry and climate. We measured H_2 fluxes at high frequency in a temperate mixed deciduous forest for 15 months using a tower-based flux-gradient approach to determine both the soil-atmosphere and the net ecosystem flux of H_2. We found that Harvard Forest is a net H_2 sink (-1.4 ± 1.1 kg H_2 ha^{-1}) with soils as the dominant H_2 sink (-2.0 ± 1.0 kg H_2 ha^{-1}) and aboveground canopy emissions as the dominant H_2 source ($+0.6 \pm 0.8$ kg H_2 ha^{-1}). Aboveground emissions of H_2 were an unexpected and substantial component of the ecosystem H_2 flux, reducing net ecosystem uptake by 30% of that calculated from soil uptake alone. Soil uptake was highly seasonal (July maximum, February minimum), positively correlated with soil temperature and negatively correlated with environmental variables relevant to diffusion into soils (i.e., soil moisture, snow depth, snow density). Soil microbial H_2 uptake was correlated with rhizosphere respiration rates ($r = 0.8$, $P < 0.001$), and H_2 metabolism yielded up to 2% of the energy gleaned by microbes from carbon substrate respiration. Here, we elucidate key processes controlling the biosphere–atmosphere exchange of H_2 and raise new questions regarding the role of aboveground biomass as a source of atmospheric H_2 and mechanisms linking soil H_2 and carbon cycling. Results from this study should be incorporated into modeling efforts to predict the response of the H_2 soil sink to changes in anthropogenic H_2 emissions and shifting soil conditions with climate and land-use change.

Keywords: atmosphere, carbon cycle, flux, hydrogen, microbe, phenology, snow, soil

Received 29 April 2016; revised version received 22 July 2016 and accepted 29 July 2016

Introduction

Soil microorganisms derive energy from the trace levels (500 ppb; nmol mol^{-1} or 1e-9 mol mol^{-1}) of H_2 in the atmosphere and drive the majority of turnover of the atmospheric burden of H_2 (1.4–2.0 year atmospheric lifetime; Novelli *et al.*, 1999; Xiao *et al.*, 2007; Ehhalt & Rohrer, 2009). Microbial scavenging of atmospheric H_2 may help supply the basal energy requirements of soil microbes, enabling nongrowing and dormant microbial cells to persist through conditions unfavorable for growth (Greening *et al.*, 2015c). While soil uptake is widely recognized as the largest sink in the H_2 budget (Ehhalt & Rohrer, 2009), it is still poorly characterized at the ecosystem level. Further constraints on the sources and sinks of atmospheric H_2 are needed to understand and predict the role of H_2 as an indirect greenhouse gas (Derwent *et al.*, 2001) and a source of water vapor to the stratosphere (Le Texier *et al.*, 1988; Tromp *et al.*, 2003; Warwick *et al.*, 2004).

Soil uptake of atmospheric H_2 is one of the least constrained components of the H_2 budget, despite being the largest of the H_2 source and sink fluxes. The global atmospheric H_2 budget includes two major atmospheric H_2 sources: photodissociation of formaldehyde (HCHO) derived from methane and nonmethane

Correspondence: Laura K. Meredith, tel. 520 626 5838, fax 520 621 9190, e-mail: laurameredith@email.arizona.edu

hydrocarbons and combustion of fossil fuels and biomass, which are nearly balanced by its two major sinks, soil consumption and oxidation by OH (Ehhalt & Rohrer, 2009; Pieterse *et al*., 2013). The largest budget terms, soil consumption (~75% of total sinks) and photochemical production (~50% of total sources), are the least well constrained with estimates ranging from 53 to 85 Tg H_2 yr^{-1} and 37 to 77 Tg H_2 yr^{-1}, respectively, across studies in recent years (Xiao *et al*., 2007; Bousquet *et al*., 2011; Yashiro *et al*., 2011; Yver *et al*., 2011a; Pieterse *et al*., 2013). Atmospheric H_2 mole fractions exhibit large year-to-year and multiyear variability, primarily driven by variability in biomass burning emissions, and have small but poorly defined multiyear growth rates (Simmonds *et al*., 2000; Langenfelds *et al*., 2002; Xiao *et al*., 2007; Grant *et al*., 2010). Anthropogenic H_2 emissions from combustion and photodissociation of HCHO derived from methane currently make up around 50% of the total H_2 source to the atmosphere (Ehhalt & Rohrer, 2009), and the anthropogenic emissions of H_2 could increase under widespread adoption of H_2 as an energy carrier, primarily due to leakage from distribution and storage systems (Tromp *et al*., 2003; Warwick *et al*., 2004). Major components of the H_2 cycle (e.g., biomass burning, soil temperature, soil moisture, and snow cover) are strongly affected by climate (Bousquet *et al*., 2011; Morfopoulos *et al*., 2012). However, uncertainty in the current balance of H_2 sources and sinks, particularly the soil sink, makes it difficult to accurately predict the impact of changes in energy use, land use, and climate on the atmospheric H_2 budget.

Quantification of the global soil flux of H_2 has relied significantly on indirect determinations using global atmospheric H_2 measurements and inverse modeling (e.g., Xiao *et al*., 2007). To better constrain H_2 fluxes, understand the microbial processes that control them, and determine the effects of climate change on these processes, additional *in situ* measurements are needed to quantify and characterize the dynamics of sources and sinks in various ecosystems. The relatively few yearlong studies of H_2 soil uptake have been performed using chamber (e.g., Conrad & Seiler, 1980; Yonemura *et al*., 2000; Lallo *et al*., 2008, 2009), inert tracer (e.g., Lallo *et al*., 2009; Schmitt *et al*., 2009; Yver *et al*., 2011b), and gradient flux (Constant *et al*., 2008b) methods. Soil chamber measurements often yield infrequent, error prone data (Hutchinson *et al*., 2000), but chamber-based results have nevertheless revealed that soil uptake depends on soil temperature and moisture, increasing to optimum values (e.g., Yonemura *et al*., 2000; Smith-Downey *et al*., 2008), and is negatively correlated with snow depth (Lallo *et al*., 2008). These data, although sparse, have been used to evaluate models of H_2 soil uptake (e.g., Morfopoulos *et al*., 2012). Relationships between H_2 uptake and soil temperature and moisture, pH, and organic content have emerged from field and laboratory studies (Smith-Downey *et al*., 2006; summarized in Constant *et al*., 2009), which have been used to construct mechanistic and statistical models (Yashiro *et al*., 2011; Ehhalt & Rohrer, 2013a,b; Morfopoulos *et al*., 2012; Khdhiri *et al*., 2015). However, additional field measurements of the H_2 soil sink are needed at sufficient temporal resolution to thoroughly evaluate models of H_2 soil uptake at the ecosystem scale. Furthermore, other components of ecosystems have not been explored as potential ecosystem sources and sinks of H_2 (i.e., no studies have partitioned soil and vegetation H_2 fluxes in an ecosystem), although various types of organic matter have been shown to emit H_2 in laboratory studies (Derendorp *et al*., 2011; Lee *et al*., 2012).

Despite the paucity of field measurements, independent advances have been made in the understanding of the genomic basis and physiology of microbial H_2 uptake (e.g., Constant *et al*., 2008a, 2010, 2011a,b; Greening *et al*., 2014). These new insights into the microbial ecology of H_2 soil cycling reveal that a diverse set of soil microorganisms harbor genes encoding for high-affinity hydrogenases that drive oxidation of atmospheric H_2 for microbial energy metabolism (Greening *et al*., 2014, 2015a). In particular, microbial scavenging of atmospheric H_2 may play a significant role during times of energy starvation and in the maintenance of dormant or nongrowing cells, which suggests that H_2 availability is important for the survival of microbial populations and their diversity in soils (Constant *et al*., 2011a; Meredith *et al*., 2014a; Greening *et al*., 2015b). Therefore, the uptake of atmospheric H_2 may be linked to the abundance of high-affinity hydrogenases in soil microbial communities and to environmental conditions triggering dormancy in soil microbial populations. Indeed, rates of soil uptake of H_2 in a diverse set of soils correlated with the number of hydrogen-oxidizing bacteria, although the optimal model included both total soil organic carbon and hydrogen-oxidizing bacteria (Khdhiri *et al*., 2015). The link between H_2 uptake and soil microbial ecology is lacking in natural systems, but would help clarify the role of H_2 uptake in the sustenance and diversity of microbial populations.

In this article, we present H_2 ecosystem fluxes measured continuously above and below the canopy of a temperate mixed deciduous forest at the Harvard Forest Long Term Ecological Research (LTER) site in Petersham, Massachusetts, from December 2010 through February 2012. We describe the factors controlling the daily, seasonal, and annual fluxes of H_2 and identify the most likely processes driving H_2 fluxes in this

ecosystem by examining a suite of environmental drivers and phenological function. We apply this extensive dataset of H_2 fluxes to increase understanding of H_2 ecosystem cycling and its biological controls in a mid-latitude forest.

Materials and methods

Site description

Measurements were made at the Harvard Forest (42.5378°, −72.1715°; elevation 340 m; Petersham, Massachusetts) Environmental Measurements Site (EMS) from December 2010 through February 2012. The site is surrounded by moderately hilly terrain that has been relatively undisturbed since the 1930s (Wofsy *et al.*, 1993; Urbanski *et al.*, 2007). The forest is mainly deciduous (80- to 115-year-old forest of red oak, red maple, red and white pine and hemlock; Barford *et al.*, 2001) and is relatively open with a top-heavy vertical distribution of foliage (Fig. S1a). Harvard Forest soil originates from sandy loam glacial till (Allen, 1995) and has relatively high levels of total carbon and nitrogen and of high-affinity hydrogenase (*hhyL*) and 16S rRNA gene copy number (Khdhiri *et al.*, 2015). Approximately 80% of fluxes measured by the EMS tower are produced within a 0.7–1 km distance from the tower, and winds come to the site predominantly from the northwest (52%) and southwest (35%), and periodically from the east (13%; Munger & Wofsy, 1999).

Flux measurements

H_2 ecosystem fluxes were measured continuously using a custom, automated flux-gradient measurement system described briefly here and in depth in Meredith *et al.* (2014b). Mole fractions of H_2, CO_2, and H_2O were measured year-round at high frequency from gas inlets installed at heights above the ground of 24 and 28 m (EMS tower above the forest canopy) and 0.5 and 3.5 m (small tower below the canopy and over undisturbed soil 14 m to the west; Fig. S1b). H_2 was measured with a gas chromatograph (Agilent, 6890, Santa Clara, CA, USA) equipped with a pulsed discharge helium ionization detector (Valco, D-3, Houston, TX, USA) and CO_2 and H_2O with nondispersive, infrared gas analyzers (LI-COR, 6262, Lincoln, NE, USA). Mole fractions were measured to high precision (0.06–0.11% for H_2, 0.025–0.043% for CO_2, and 0.04–0.05% for H_2O) and were calibrated against H_2 and CO_2 standards traceable to National Oceanic and Atmospheric Administration (NOAA) Earth System Research Laboratory Global Monitoring Division (ESRL/GMD) primary standard scales. We used well-mixed integrating volumes to smooth out temporal fluctuations in mole fractions occurring at a higher frequency than our ability to measure their vertical gradients (details in Sec. 2.4.2 of Meredith *et al.*, 2014b). Routine null bias tests were used test that no bias existed (offsets in measured mole fractions) between gas inlets (Sec. 2.4.3, Meredith *et al.*, 2014b). Independent eddy covariance CO_2 and H_2O flux measurements were made above the forest canopy at a height of 29 m (Munger & Wofsy, 1999; Urbanski *et al.*, 2007). Sonic anemometers installed at 2 m and 29 m measured 3-dimensional wind speeds.

H_2 fluxes were determined with flux-gradient methods evaluated in Meredith *et al.* (2014b) and applied here to present the first H_2 ecosystem flux results at this site. The flux-gradient method assumes a proportional relationship between trace gas fluxes, F, and their vertical (z) concentration gradients ($\Delta[H_2]/\Delta z$) scaled by the rate of turbulent exchange or eddy diffusivity, k: $F = -k\Delta[H_2]/\Delta z$. Briefly, we used two flux-gradient approaches to infer k by (i) similarity to the flux and gradient of other trace gases (Modified Bowen Ratio) or (ii) parameterization of the eddy diffusivity (k parameterization). We have shown that fluxes of CO_2, H_2O, and carbonyl sulfide (COS) determined with the flux-gradient approach at the EMS site were consistent with independent measurements of the same trace gas fluxes determined by eddy covariance or soil chambers (Meredith *et al.*, 2014b; Commane *et al.*, 2015). We excluded data from periods with rain, poorly developed turbulence, exceedingly small mole fraction gradients in the denominator, and unrealistic values for the inferred turbulent diffusion coefficient (Appendix S1; Meredith *et al.*, 2014b). The filtered dataset represents 26% and 35% of the half-hourly measurements in 2011 for above- and below-canopy measurements, respectively. This work yields the first measurement-based estimate of the total H_2 flux of a mid-latitude forest.

In this article, we use a subscript notation for tower-based trace gas flux measurements (F) to denote the trace gas species, H_2 (F_{H2}) and CO_2 (F_{CO2}), and the flux location, soil-atmosphere (F_S), net ecosystem (F_E), and aboveground (F_A). Soil-atmosphere fluxes were measured for H_2 ($F_{H2,S}$) and CO_2 ($F_{CO2,S}$) below the canopy at 2 m above the forest floor; little to no subcanopy vegetation was present in the footprint of below-canopy measurements. Net ecosystem fluxes were measured above the canopy at 26 m and 29 m height for H_2 ($F_{H2,E}$) and CO_2 ($F_{CO2,E}$), except in the winter when the net ecosystem flux was small and was instead derived from the 2 and 26 m gradient (Fig. S2). Aboveground fluxes of H_2 ($F_{H2,A}$) were calculated as the difference between net ecosystem and soil fluxes ($F_{H2,E} - F_{H2,S}$) and represent the H_2 flux between 2 and 26 m. Negative values of trace gas fluxes indicate trace gas uptake by the soil, ecosystem, or aboveground components from the atmosphere, while positive fluxes indicate emissions to the atmosphere. In addition to the flux, we also calculated the concentration-independent uptake rate of H_2 (H_2 deposition velocity, $v_d = -F_S/[H_2]$; cm s^{-1}), to account for differences in ambient H_2 that can influence first-order uptake rates. Data available from the Harvard Forest Data Archive (Meredith, 2016).

We used automated soil chambers to measure CO_2 respiration rates (R) from the forest floor approximately 0.6 km south of the EMS tower with similar soils and vegetation (Sec. 2.2, Meredith *et al.*, 2014b). This custom-made automated soil respiration measurement system consisted of an infrared gas analyzer (IRGA, LI-7000, LI-COR Inc., Lincoln, NE, USA) and six automated soil chambers (20 cm in diameter) (J. Tang, *personal communication*). The system included three control plots

measuring total soil respiration (R_S) and three additional trenched plots (i.e., roots severed to measure non-root-associated respiration by heterotrophic microbes; R_H) to exclude autotrophic respiration by roots and root-associated microbes (R_A). Autotrophic respiration (sometimes called rhizosphere respiration) was calculated from the difference between control and trenched plots: $R_A = R_S - R_H$.

Plant and environmental data and analysis

Environmental data in these analyses included meteorological data (Boose, 2001), carbon, water, and energy fluxes (Munger & Wofsy, 1999) and sap flow (related to transpiration) measurements (reported in Commane *et al.*, 2015) at the EMS site or nearby sites within Harvard Forest. To characterize the sensitivity of H_2 fluxes to environmental variables, we used an artificial neural network (ANN) method on 30-min data for soil-atmosphere fluxes ($F_{H2,S}$) and on 4-day low-pass filtered H_2 fluxes for net ecosystem H_2 fluxes ($F_{H2,E}$) following methods described in Shoemaker *et al.* (2014). We report averaged fluxes and their uncertainty (±) with 95% confidence intervals. The level of statistical significance is indicated with *P*-values. Time is reported as Eastern Standard Time (EST).

Snow depth (SD) was determined from the number of stripes visible on five painted graduated snow stakes (PVC with alternating vertical red and white stripes of 5 cm height) distributed within the field of vision of the subcanopy webcam mounted on the EMS tower (Fig. S3) that takes images every 30 min during daylight hours (Richardson, 2008). The snowpack water content (snow water equivalent, SWE) was continuously measured in a nearby forest stand (+42.53°, −72.19°, alt 340 m) (Boose, 2009). Snow porosity (percent air-filled space) was determined from SWE and SD as (1 - SD/SWE) × 100% and represents an average bulk porosity of the snow profile. Data available from the Harvard Forest Data Archive (Meredith, 2016).

Site phenology was assessed using automated repeat digital imagery with PhenoCam images taken from the Harvard Forest EMS tower. In contrast to the abrupt start of the growing season, senescence and leaf abscission display more gradual, heterogeneous timing of phenology across plant species and individuals within the forest (Richardson *et al.*, 2009; Gill *et al.*, 2015). To better characterize the senescence period, we identified the date of maximum redness, as quantified by the redness chromatic coordinate, for the different locations in the PhenoCam image field of view (Fig. S4). For details on this type of analysis, see Richardson *et al.* (2009) and Klosterman *et al.* (2014). We defined a senescence index as the cumulative sum of the locations in the image that had reached maximum redness (see also Yang *et al.*, 2014), and the senescence index was used as a measure of the percentage of total senescence that had occurred at any point in time. The senescence index and curve fitting methods (Klosterman *et al.*, 2014) were used to classify the study period into three types of forest-wide phenological seasons: growing, senescent, and dormant with the following phenological transition dates for 2011: May 3 for start of spring, October 2 for start of fall senescent period, and November 12 for end of fall and beginning of the dormant season. These dates were consistent with ground-based phenological observations of leaf coloration and leaf fall (O'Keefe, 2011) and sap flow (Commane *et al.*, 2015).

Results

Seasonal dynamics of H_2 fluxes

At Harvard Forest in 2011, we observed a net annual flux of H_2 into the ecosystem from the atmosphere (-1.4 ± 1.1 kg H_2 ha^{-1}) with soils as the dominant H_2 sink (-2.0 ± 1.0 kg H_2 ha^{-1}) and aboveground emissions from the forest canopy as the dominant source ($+0.6 \pm 0.8$ kg H_2 ha^{-1}). The soil-atmosphere flux ($F_{H2,S}$) and concentration-independent flux (deposition velocity, v_d) of H_2 show greatest monthly mean soil uptake rates during summer and fall, rapidly peaking in July ($F_{H2,S}$ -7.9 ± 0.3 nmol m^{-2} s^{-1}; v_d 0.043 ± 0.002 cm s^{-1}; Fig. 1a, b) coincident with the mean monthly maximum in soil and air temperature (Fig. 1c), minimum in soil moisture (Fig. 1c), and maximum in soil CO_2 respiration rates ($F_{CO2,S}$) (Fig. 1d). H_2 soil uptake rates fell slowly through the fall and persisted at low values in winter and spring with lowest values in February 2011 (-0.46 ± 0.1 nmol m^{-2} s^{-1}; 0.003 ± 0.001 cm s^{-1}). Despite the strongly contrasting snow depth and air temperature patterns between the two winters within the measurement period (Fig. 1c), wintertime $F_{H2,S}$ was not statistically different between these years, although there was a statistical difference in the CO_2 efflux. The net H_2 ecosystem flux was primarily driven by soil uptake, except during the period of leaf senescence when aboveground emissions of H_2 outpaced soil uptake, leading to a positive net ecosystem H_2 flux ($+8.4 \pm 6.9$ nmol m^{-2} s^{-1}) coincident with the forest shifting from a net sink to a net source of CO_2 (i.e., when ecosystem respiration (R_{eco}) outweighed gross ecosystem productivity (GEP), Fig. 1d). Thus, the balance in bidirectional exchange of H_2 by soil and aboveground processes shifted seasonally at the Harvard Forest between a net sink and source of atmospheric H_2, as is the case for CO_2.

Environmental drivers of soil fluxes of H_2

The 2011 spring and summer represented typical environmental conditions for Harvard Forest (Appendix S2), while the fall and winter were wetter and warmer than recent climatology (defined here as from 2001 through 2012 using data from Boose, 2001). Over the study period, air temperatures ranged from −26 °C (December 2010) to 36 °C (July 2011), which were the minimum and maximum 30-min averaged extremes over the 12-year recent climatology. Soil

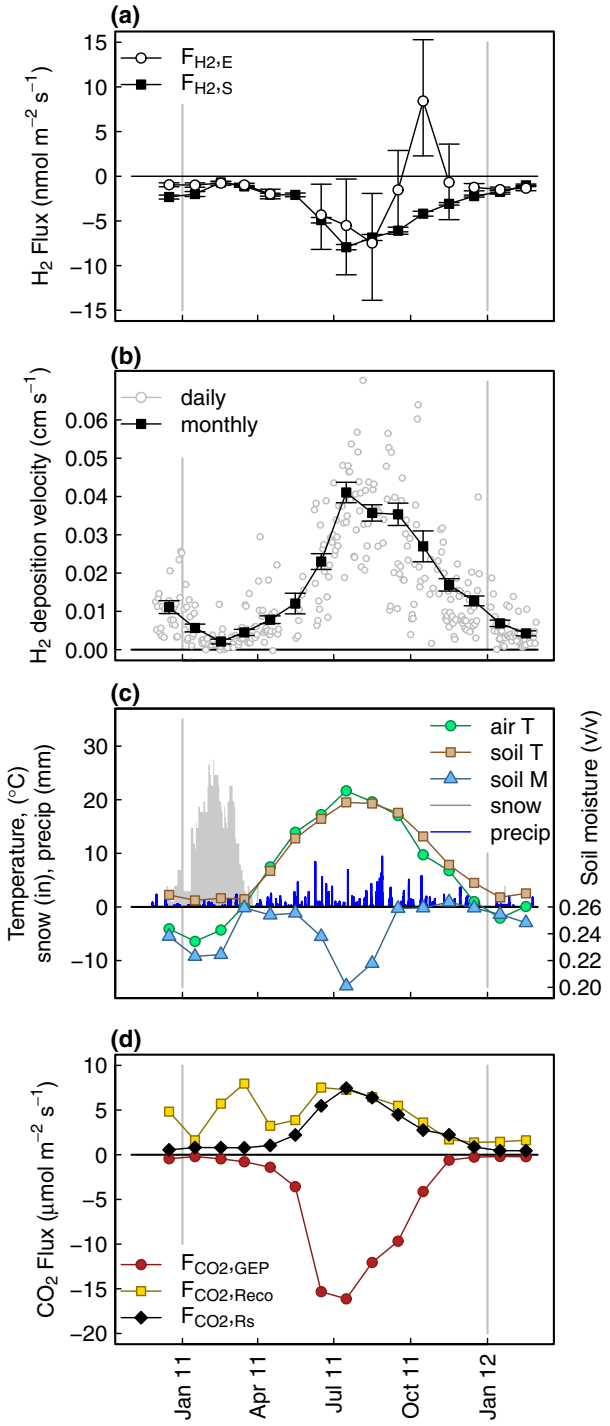

Fig. 1 H_2 cycling at the Harvard Forest was primarily driven by soil uptake with similar seasonality to environmental variables and carbon fluxes, and net ecosystem emissions of H_2 became significant during the fall. The (a) daytime (0900–1700 EST) monthly mean H_2 net ecosystem ($F_{H2,E}$) and soil-atmosphere flux ($F_{H2,S}$) mainly reflected the soil sink until they diverged statistically in October. The (b) monthly (●) and daily (o) H_2 deposition velocity (v_d) exhibited strong seasonality and daily variability. Concurrent (c) mean monthly environmental variables: air temperature (air T), soil temperature (soil T), and soil moisture (soil M) and 30-min averaged snow depth (snow; gray shading) and precipitation (precip; blue lines). The (d) mean monthly gross ecosystem productivity (GEP), ecosystem respiration (R_{eco}), and soil respiration (R_s) highlight the bidirectional nature of CO_2 fluxes. Monthly averages plotted on day 15 of each month and vertical bars represent 95% confidence intervals.

temperature ranged from 0 to 25 °C, and soil moisture measured at a well-drained location in the forest ranged from 9.8% to 25.7% and from 21.0 to 51.1% at a relatively poorly drained location. We include soil moisture from both locations to capture the range of variability in soil moisture temporal responses (i.e., dry sites typically drain faster, while wet sites retain moisture longer) present at the field site during the period we made H_2 measurements. Monthly mean air temperature, soil temperature, and soil moisture were not significantly different from the recent climatology during the spring and summer months (Figs S5 and S6). Precipitation began to recharge soil moisture relatively early (August) from the summertime minimum and summed to make 2011 the wettest in recent climatology with 162 cm of cumulative precipitation and above average soil moisture in the fall and winter. The site experienced two extreme events, Hurricane Irene on August 28, 2011, and an early season snowstorm on October 29, 2011, which brought 111 cm and 26 cm of precipitation as rain and snow, respectively (Boose, 2001). Compared to the recent climatology, the 2010–2011 winter was cold (December–January–February (DJF) mean air temperature: −4.9 °C) and had a deep snowpack (75 cm max) that persisted until April 07, 2011, while the 2011–2012 winter was warm (DJF mean air temperature: −0.7 °C) and had a thin short-lived wintertime snowpack (16 cm max) and most precipitation fell as rain (Fig. S6). These two distinct winters allowed us to compare the effect of contrasting winter conditions on H_2 fluxes at the Harvard Forest.

Given their importance in previous studies, we first evaluated soil temperature and moisture as potential drivers of H_2 uptake rates at Harvard Forest. H_2 uptake increased with soil temperature (Fig. 2a; $r = 0.66$, $P < 0.001$) and decreased with increasing soil moisture levels (Fig. 2b; $r = -0.48$, $P < 0.001$ and $r = -0.39$, $P < 0.001$ for moisture probes in comparatively dry and wet sites, respectively). The dependence of v_d on soil temperature and moisture exhibited a broad maximum in uptake at temperatures of approximately 17 °C and below soil moisture levels of 17% and 33% at the dry and wet site, respectively (Fig. 2c, d). From this

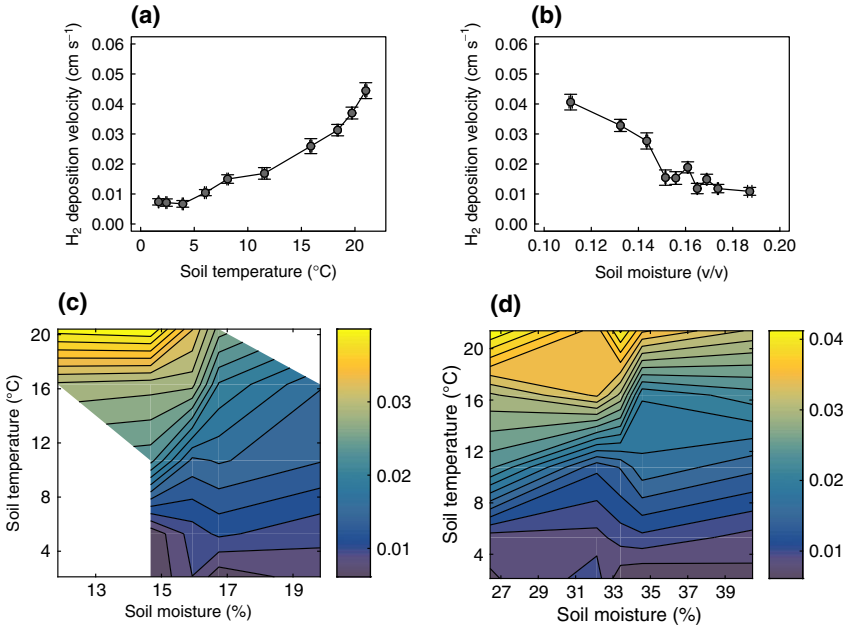

Fig. 2 H_2 soil uptake increased with soil temperature (at 10 cm depth) and decreasing soil moisture. Quantile plots of the mole-fraction normalized flux (v_d, deposition velocity) of H_2 increased with (a) soil temperature ($r = 0.66$, $P < 0.001$) and (b) decreasing soil moisture ($r = -0.48$, $P < 0.001$, comparatively dry site shown here). H_2 deposition velocity (color bar in cm s^{-1}) was highest at warm temperature and low soil moisture conditions measured by soil moisture probes at relatively dry (c) and wet (d) sites.

maximum, soil H_2 uptake dropped steeply until reaching low levels of v_d with less sensitivity to temperature and moisture at low temperature (<8 °C) regardless of soil moisture level. H_2 soil uptake at Harvard Forest was sensitive to soil temperature and moisture, particularly at warmer temperatures.

The potential for other environmental variables to explain soil fluxes of H_2 was evaluated using an artificial neural network (ANN) multivariate statistical analysis on half-hourly fluxes. As in the linear correlation analysis above, soil temperature and soil moisture (relatively dry site) emerged as top predictors of soil uptake rates of H_2 (Fig. 3a), respectively, explaining 68% and 54% of the variance in H_2 soil fluxes. Soil moisture measured at the relatively drier site was a better predictor of H_2 soil fluxes than the wetter site (54% dry; 46% wet). The ecosystem fluxes of CO_2 were also significant predictors of H_2 soil fluxes; net ecosystem exchange (NEE) and gross ecosystem productivity (GEP) explained 52% and 49% of the variance in H_2 soil fluxes, respectively (Fig. 3a). Using all the predictor variables in Fig. 3a, the ANN model explained 76% of the variability observed in annual H_2 fluxes. Sap flow was not evaluated in the annual model because these data were limited to the growing and senescent seasons, but during those periods, sap flow explained as much variability in H_2 soil fluxes as soil temperature. The observed and ANN modeled H_2 soil fluxes (Fig. 3b) agreed well, especially during the growing season, while the largest relative model-data mismatch occurred during the winter (Fig. 3c).

The ANN analysis revealed a statistically significant relationship between rates of soil-atmosphere exchange of H_2 and CO_2, which we then investigated by comparison of $F_{H2,S}$ to automated chamber measurements of soil respiration (R). The chambers measured total soil respiration (R_S), which is the sum of the respiration of soil organic matter (heterotrophic, R_H) and the (rhizosphere) respiration by roots and root-associated microbes of recently photosynthetically fixed carbon (autotrophic, R_A). H_2 uptake by soils correlated more strongly (Fig. 4) with total soil respiration ($Rs = R_A + R_H$, $r = -0.74$, $P < 0.001$) and rhizosphere respiration (R_A, $r = -0.80$, $P < 0.001$), than non-root-associated respiration measured in 'trenched' plots (R_H, $r = -0.54$, $P < 0.001$). In other words, H_2 soil uptake was more strongly related to carbon fluxes derived from recent photosynthates than carbon fluxes driven by microbial communities respiring independently of root exudates.

The 15-month period of our study allowed us to study the effects of H_2 uptake during two very different winters: the cold 2010–2011 winter with enduring snow, as is typical for this New England site, vs. the warm and wet 2011–2012 winter (Fig. 1c). Snow insulation in January and February of 2010–2011 compensated for colder air temperatures (-5.4 ± 0.2 °C in 2010–2011; -1.6 ± 0.2 °C in 2011–2012) leading to

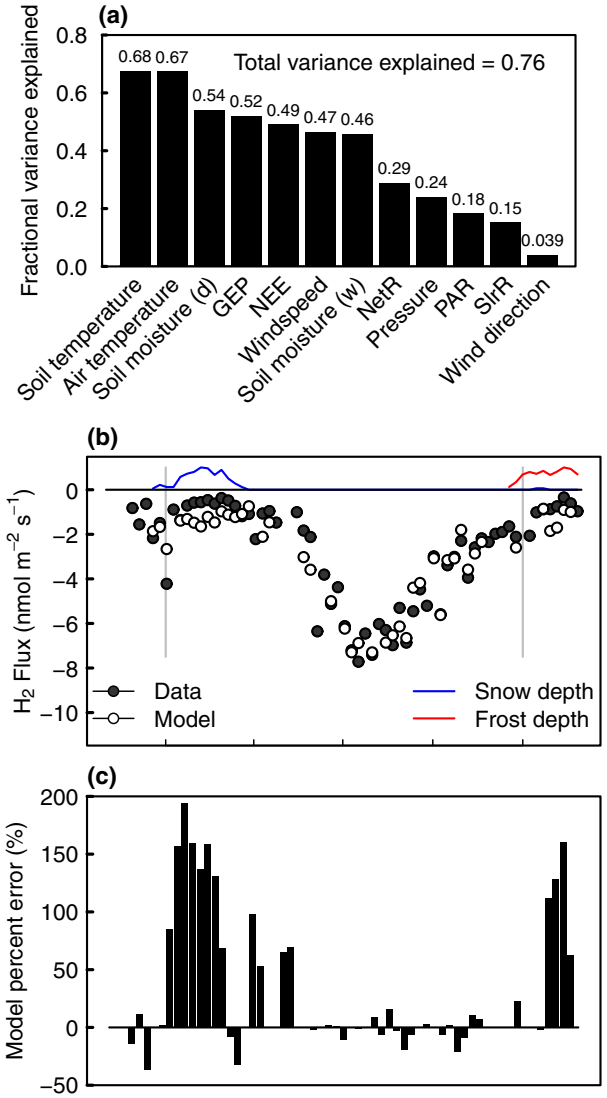

Fig. 3 Multivariate statistical analysis revealed that (a) in addition to temperature and soil moisture, GEP and NEE and other environmental drivers combined to explain up to 76% of the variance in annual H_2 soil fluxes. Comparison of (b) four-day measured (data) H_2 soil fluxes and ANN results (model) with the (c) relative model-data mismatch show good agreement during most of the year, until the winter time. Snow depth (blue line) and frost (red line; data not available in 2010–2011) were not included in the model, which likely reduced $F_{H2,S}$ below levels that would have been predicted based on the (a) modeled environmental drivers. The periods with snow and frost are represented qualitatively in (b).

similar wintertime soil temperatures (1.4 ± 0.01 °C; 2.1 ± 0.03 °C). The soils were drier in the winter of 2010–2011 (14.8 ± 0.01%; 16.0 ± 0.1% dry site, and 30 ± 0.02%; 34.3 ± 0.1% wet site) because precipitation was locked up in snow. With snow, $F_{H2,S}$ was not sensitive to changes in soil temperature or moisture

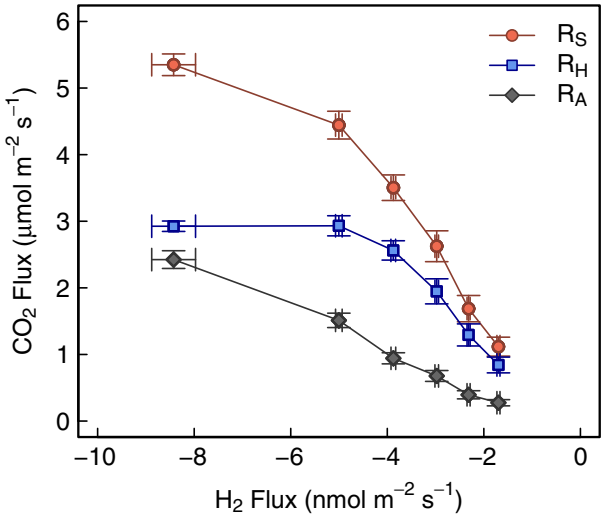

Fig. 4 The H_2 soil flux correlated with total soil respiration (R_S) and rhizosphere respiration (R_A) more strongly than heterotrophic soil microbial respiration (R_H). Annual data are partitioned to have equal numbers of H_2 flux data points averaged per plot symbol.

($P > 0.5$). Instead, $F_{H2,S}$ was affected by snow and its resistance to trace gas diffusion: v_d decreased with increasing depth of snow ($r = -0.36$, $P < 0.001$) and decreasing snow porosity ($r = 0.33$, $P < 0.001$) (Fig. 5). In contrast, soil respiration ($F_{CO2,S}$) was more strongly affected by soil temperature ($r = 0.32$, $P < 0.001$) than snow depth ($r = 0.09$, $P < 0.001$) and porosity ($r = -0.01$, $P > 0.5$). Thus, diffusion limitation by snow

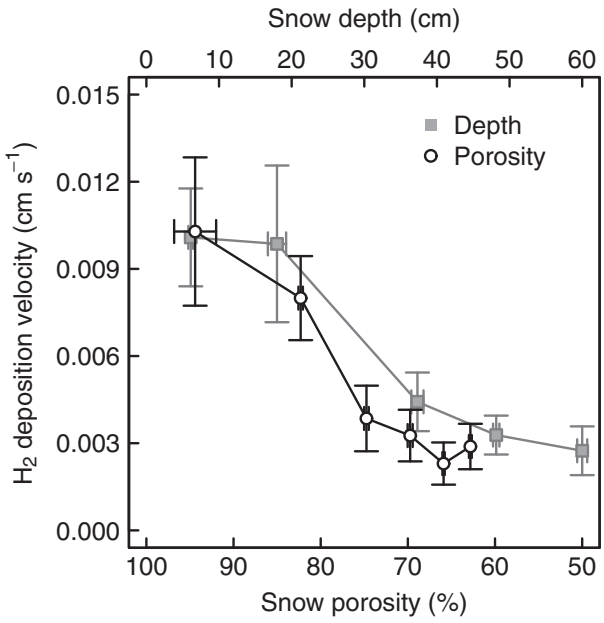

Fig. 5 Soil uptake of H_2 persisted even in the presence of snow but at a diminished rate. The H_2 deposition velocity decreased with increasing snow depth and with decreasing snow porosity.

decreased uptake of H_2 but did not strongly affect emission of CO_2. In the winter of 2011–2012, the absence of snow allowed upper layers of the soil to freeze, and the depth of freezing (down to 10 cm) was a significant factor in reducing both v_d ($r = -0.14$, $P < 0.001$) and $F_{CO2,S}$ ($r = -0.18$, $P < 0.001$). These factors combined to no yield significant difference in $F_{H2,S}$ between the snow and snow-free winters ($P = 0.95$), but greater $F_{CO2,S}$ during January and February of 2011–2012 than 2010–2011 (0.83 ± 0.04 vs. 0.45 ± 0.02 umol m^{-2} s^{-1}, $P < 0.001$).

Aboveground emissions dominated H_2 ecosystem fluxes during senescence

Aboveground H_2 fluxes ($F_{H2,A}$) were calculated as the difference between the ecosystem and soil fluxes and represent H_2-producing or H_2-consuming processes in the forest canopy and other aboveground biomass (between 3.5 m and 24 m height above the forest floor). Aboveground H_2 fluxes varied with forest-wide phenological transitions punctuating the growing, senescent, and dormant periods. Daytime $F_{H2,A}$ were negligible during the growing season (+1.4 ± 3.0 nmol m^{-2} s^{-1}) and dormant season (+0.4 ± 1.4 nmol m^{-2} s^{-1}), but increased significantly during senescence (+13.2 ± 5.0 nmol m^{-2} s^{-1}), overwhelming uptake by soils during that period ($F_{H2,S} = -5.7 \pm 0.6$ nmol m^{-2} s^{-1}), and converting this mixed deciduous forest into a net source of H_2 ($F_{H2,E} = +7.5 \pm 4.9$ nmol m^{-2} s^{-1}) (Fig. 1a). $F_{H2,A}$ was negligible at night (+0.9 ± 20 nmol m^{-2} s^{-1}) indicating that the senescing forest transitioned between a net ecosystem source and sink of H_2 on a diurnal basis. Annual aboveground H_2 emissions (+0.6 ± 0.8 mg H_2 ha^{-1} a^{-1}) made up 22% of the annual gross H_2 ecosystem fluxes, reducing the net ecosystem uptake by 30% of what would have been deduced by considering soil uptake alone. Aboveground emissions of H_2 were an unexpected, yet significant component of the H_2 cycling on both a seasonal and annual basis at the Harvard Forest.

Aboveground emissions of H_2 were temporally and spatially related to senescing deciduous trees. These emissions occurred during senescence (>40 day period) and originated between heights of 3.5 m and 24 m, where approximately 96% of the foliar density is located (Fig. S1). Deciduous trees at our site began to change color in early September (Fig. 6a, senescence index > 0). Maple and birch (4 : 1 abundance in terms of basal area at the site, D. Orwig, personal communication) senesced rapidly between October 4 to 19 (15% of measured forest senescence), while oak senescence was more slow and heterogeneous, proceeding from October 19 to November 12 (100% senescence) (Fig. S4). No significant difference in the H_2 flux between these two periods was observed, although some data were missing during oak senescence. In contrast, net ecosystem exchange of CO_2 was lower during oak senescence than during maple senescence (−9.1 vs. −0.9 μmol m^{-2} s^{-1}) indicating that photosynthetic rates were dropping over the course of forest senescence. $F_{H2,A}$ emissions correlated with wind direction ($P < 0.01$), and larger emissions were observed from the west (Fig. 6b), particularly at longer fetches sampled by higher wind

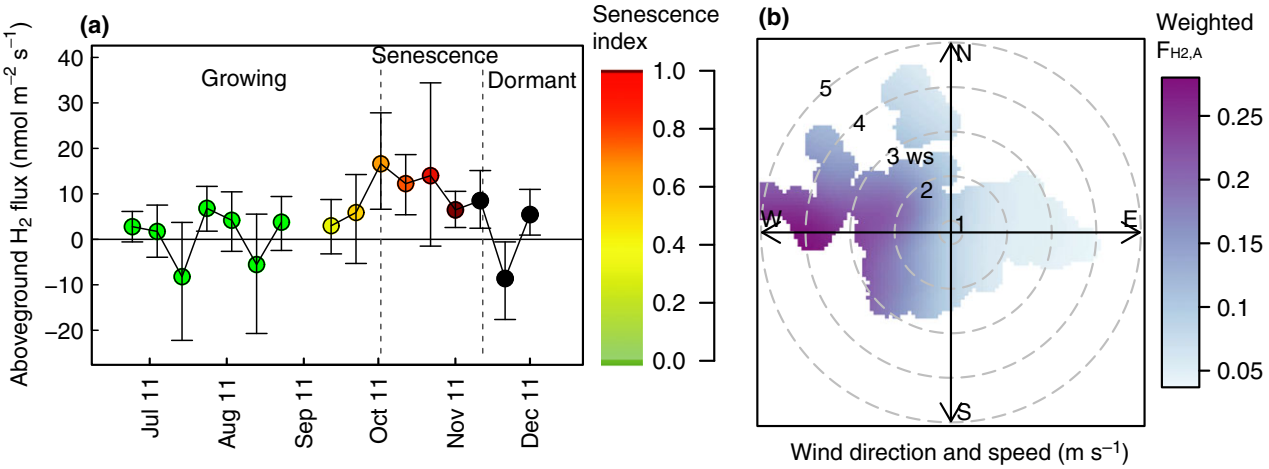

Fig. 6 Daytime (900–1700 EST) aboveground H_2 fluxes ($F_{H2,A}$) reveal H_2 emissions during forest senescence from sectors dominated by deciduous trees. The emissions were sustained throughout senescence as shown in (a) by the 10-day average $F_{H2,A}$ (bars indicate 95% confidence intervals). Points are colored by the PhenoCam-derived senescence index to show the fractional progression of senescence from the growing season (0, light green) to the dormant season (1, black) as indicated by the color bar. Emissions originated in sectors to the west as shown in the wind rose (b) with the highest frequency-weighted emission observations in the section (west–northwest and southwest) dominated by deciduous trees (openair R package; Carslaw & Ropkins, 2012).

speeds. The flux tower footprint contained mixed deciduous conifer forests in all directions, but with greater dominance of deciduous trees to the southwest and beyond 200 m to the west–northwest. To the east, conifers and current or drained ponds dominate the landscape.

Ecosystem fluxes of H_2 were highly variable as a result of the low signal to noise of the measurement and variability in the balance between H_2-producing and H_2-consuming processes. We performed multivariate ANN analysis on 4-day averaged daytime $F_{H2,E}$ values, which revealed that maple sap flow explained the most variability (approximately 70%) out of the tested environmental drivers (Fig. S7). ANN results differed for $F_{H2,E}$ derived by a single flux-gradient approach (trace gas similarity using CO_2) and for $F_{H2,E}$ derived by merging with a second flux-gradient approach (trace gas similarity using H_2O). The total variability explained was 63% and 82% in the former vs. the latter, and besides sap flow, environmental drivers were not always consistent between the two flux calculations (comparison in Fig. S7). In general, ANN results suggested that 4-day averaged fluxes were related to maple sap flow, soil moisture, CO_2 fluxes (GEP and NEE), and radiation (net and photosynthetically active), which were trends seen also in quantile plots (Fig. S8). These results may help point to environmental drivers for net ecosystem fluxes of H_2 and aboveground H_2 emissions.

Discussion

Soil uptake of H_2

Soil uptake of H_2 in this mixed deciduous forest was seasonal (July maximum, February minimum) and varied by more than ten-fold in monthly mean v_d (0.003 to 0.043 cm s^{-1}; Fig. 1b). The relatively few yearlong studies of H_2 soil uptake in the past report similar v_d seasonality (summer/fall maximum, winter/spring minimum) and magnitude (typically between 0.01 and 0.1 cm s^{-1}) (Conrad & Seiler, 1980; Yonemura *et al.*, 2000; Constant *et al.*, 2008b; Lallo *et al.*, 2008, 2009; Yver *et al.*, 2011b). Soil H_2 uptake rates are typically high in forests soils relative to other ecosystems such as grasslands (Ehhalt & Rohrer, 2009; Constant *et al.*, 2011b; Khdhiri *et al.*, 2015). The annual average deposition velocity at Harvard Forest (0.02 cm s^{-1}) was lower than some values reported from chamber-based measurements in forests (0.063 and 0.15 cm s^{-1}) (Förstel, 1988; Förstel & Führ, 1992; Yonemura *et al.*, 2000) and global estimates derived from the H_2 soil sink budget term (0.036–0.052 cm s^{-1}) (Ehhalt & Rohrer, 2009). Although Harvard Forest soils exhibited some of the highest H_2 uptake rates per unit mass in a recent laboratory-based survey of soils (Khdhiri *et al.*, 2015), *in situ* H_2 uptake rates depend on soil bulk density (i.e., conversion to H_2 uptake per unit area) and diffusional barriers to trace gases soil uptake (Ehhalt & Rohrer, 2013a) and may be lower in the field relative to other sites. H_2 uptake rates at Harvard Forest were affected by *in situ* diffusion limitations on v_d such as from soil water saturation, snow, and perhaps inactive soil or litter layers (Smith-Downey *et al.*, 2008; Ehhalt & Rohrer, 2013a,b). Indeed, models representing diffusion limitation mechanisms (Yashiro *et al.*, 2011; Morfopoulos *et al.*, 2012) agree well with the seasonality and magnitude of our H_2 soil uptake observations at Harvard Forest, which represent the most extensive soil-atmosphere flux measurements to date available for model evaluation.

H_2 soil uptake rates were sensitive to temperature and soil moisture, consistent with underlying biological and physical mechanisms. H_2 soil uptake increased with soil and air temperature as expected for an enzyme-mediated process. Optimum temperatures of approximately 30 °C for soil H_2 uptake (Ehhalt & Rohrer, 2011) were rarely exceeded in this study (i.e., <2% of the days in 2011), so the temperature response of H_2 uptake was consistently positive. H_2 soil uptake decreased with soil saturation, as water-filled pore spaces impede gas diffusion (Conrad & Seiler, 1981; Smith-Downey *et al.*, 2006). Soil moisture did not drop below minimum levels required for biological activity (e.g., <1% in desert soils; Smith-Downey *et al.*, 2008); thus, no soil moisture optimum was observed in our Harvard Forest data, so the moisture response of H_2 uptake was consistently negative. Our *in situ* observations were consistent with patterns observed in laboratory-based measurements of the temperature and moisture dependence of H_2 soil uptake (e.g., Smith-Downey *et al.*, 2006). Soil moisture levels were above average from August 2011 through the end of the study period, which may have reduced annual H_2 soil uptake. Thus, soil uptake in 2011 could be considered a lower estimate for typical years at Harvard Forest. Temperature and moisture were the primary controls on H_2 soil uptake in this study. Changes to soil moisture and temperature with global change should affect patterns and the magnitude of the global H_2 soil sink.

We expected H_2 soil uptake to differ strongly across the two contrasting wintertime regimes, but compensating processes resulted in indistinguishable differences between wintertime $F_{H2,S}$ in these two years. In 2010–2011, snow insulated soils against freezing air temperatures, yet permitted diffusion of H_2 through the snow matrix, thereby playing a critical role in allowing H_2 uptake by the subnivean soil microbial community. Soils in the 2010–2011 winter were drier (by around 4%) and only slightly colder (by <1 °C) than

in the 2011–2012 winter (Fig. 1c). Given the greater sensitivity of H_2 uptake to moisture (Fig. 2b; 30–34%) than temperature (Fig. 2a; 1–2 °C), we expected higher H_2 uptake rates in the 2010–2011 winter than in 2011–2012. Indeed, the ANN model predictions (Fig. 3b), which did not account for snow or frost depth, estimated higher rates of H_2 uptake during the 2010–2011 winter than were actually observed (overestimated by more than 100%; Fig. 3c) illustrating that H_2 soil uptake was reduced below our expectations based on ecosystem properties such as soil moisture and temperature. Snow reduces rates of H_2 soil uptake as compared to snow-free periods by adding resistance to H_2 diffusion. Concentration gradients establish in the snow, suppressing H_2 mole fractions at the soil surface, thereby reducing concentration-dependent first-order H_2 uptake rates. Snow depth and porosity were the primary factors controlling H_2 soil uptake rates during snow-covered periods (see also Lallo *et al.*, 2008, 2009). In contrast, soil respiration rates were insensitive to CO_2 buildup, and soil temperature and moisture controlled wintertime respiration rates under snow. In the 2011–2012 winter, soils lacked snow cover and therefore froze, which reduced rates of both $F_{H2,S}$ and R_s. These results reveal complex mechanistic controls on dormant season H_2 fluxes, which comprised a significant portion (35%) of the H_2 soil uptake at Harvard Forest in 2011.

Over the next century air temperatures in winter are projected to rise, winter precipitation as snow is expected to decrease in depth and duration, and soil freeze–thaw cycles are expected to rise in frequency in this region (Hayhoe *et al.*, 2007). To aptly project the impact of these climatic changes on H_2 soil uptake in this region and beyond, models should account for persistence of H_2 uptake through snow, insulating properties of snow for soil microbial communities, and the selective impact of diffusion resistance on H_2 uptake reactions over production reactions, which may also be extended to other trace gases.

H_2 energy flux to soil microbial communities

The dominant process driving the soil H_2 sink is aerobic consumption of atmospheric H_2 by soil microorganisms harboring high-affinity [NiFe]-hydrogenases (Greening *et al.*, 2015c). We did not observe net emissions of H_2 from soils that would indicate fermentative degradation of organic matter (e.g., Yonemura *et al.*, 2000) or high levels of nitrogen fixation (Conrad & Seiler, 1980). H_2 soil uptake was found to covary with stages of forest phenology (i.e., growing, senescent, and dormant seasons; Fig. 1b), carbon cycling (i.e., GEP, NEE; Fig. 3a), autotrophic or root-associated microbial respiration (R_A; Fig. 4), and sap flow (decreases during senescence). Microbial communities associated with R_A are metabolically linked to plant photosynthesis and may be strongly controlled by root interactions, while the microbial communities involved in R_H are influenced by non-root-associated soil interactions (Savage *et al.*, 2013). These microbial communities may differ in terms of activity, community composition, and ecology (Philippot *et al.*, 2013). Nitrogen fixation releases H_2 during N_2 reduction by nitrogenase, which can then be emitted to the local environment and to the atmosphere if not consumed in the soil. Free-living microbes or roots supporting nitrogen-fixing nodules (e.g., legumes, clover, alders, red pines) can thus be a subterranean source of H_2, potentially influencing soil microbial community composition and rates of soil H_2 fluxes and CO_2 fixation (Dong & Layzell, 2001; Stein *et al.*, 2005; Maimaiti *et al.*, 2007; Osborne *et al.*, 2010; Piché-Choquette *et al.*, 2016). Biological nitrogen fixation is however not a significant component of the N budget in N-limited forests at Harvard Forest (Tjepkema, 1979) although microorganisms harboring the *nifH* (nitrogenase reductase) gene for N_2-fixation are present (Compton *et al.*, 2004). As a result, we suspect that the association between R_A and $F_{H2,S}$ is unlikely to be related to N_2 fixation at this site. The relationship could instead arise from increased availability of rhizodeposits (e.g., nutrients, exudates, mucilage released by the plant root) and preferential enrichment of H_2-consuming microbes in the rhizosphere microbiome, such as Actinobacteria (Philippot *et al.*, 2013).

Atmospheric H_2 consumption by microorganisms to fuel their energy metabolism may play a key role in survival of a diverse microbial population during periods of environmental hardship (Constant *et al.*, 2011b; Meredith *et al.*, 2014a; Greening *et al.*, 2015a). H_2 represents a widespread and dependable mode of delivery of electrons to the microbial respiratory chain during energy starvation (King, 2003). We therefore consider trace gas fluxes of H_2 and CO_2 to reflect microbial energy metabolism by oxidation of H_2 and respiration of carbon substrates, respectively. At Harvard Forest, annual soil H_2 uptake provided 0.25 mol ATP m^{-2} of energy to the soil microbial population, which is 0.11% of the total energy derived independently from carbon substrates from heterotrophic respiration (R_H, 180 mol ATP m^{-2}) and the microbe-mediated portion of autotrophic respiration (R_A, 40 mol ATP m^{-2}; calculations in Appendix S4). While smaller than from carbon, H_2 energy can meet the maintenance energy demands of 10^6 to 10^7 H_2-oxidizing microbes per gram of soil or approximately 0.1% of the total microbial population (Constant *et al.*, 2010). The estimated energy flux from H_2 vs. carbon substrates varied with forest phenology. A greater proportion of the annual energy supplied

from H_2 was derived during the dormant and senescent seasons (35% of annual energy from H_2) over the same period (22% of annual energy from carbon substrate respiration). Carbon substrate respiration was relatively weighted more heavily toward the growing season (Fig. 7). Of the annual microbial maintenance energy demand (m_E; Appendix S4 following Conrad (2006)), approximately 30% occurred in the dormant and senescent seasons (Table S1). H_2 oxidation may be an important component of microbial energy metabolism outside of the growing season. We estimated the ratio of the population size of microbes that could be supported by H_2 oxidation vs. that supported by carbon substrate respiration (Appendix S4), which increased by a factor of 2.5 from the growing (July 2011; 0.76%) to the dormant season (January 2012; 1.9%). Thus, H_2 may help maintain microbial populations experiencing a reduced supply of carbon substrates and lower temperatures during the dormant and senescent season. Diffusional constraints to H_2 reaching soils (e.g., by water, snow) may reduce the ability of microbes to access atmospheric H_2 energy, representing a potential H_2-mediated link between changes in climate (shifts in snow and precipitation regimes) and soil microbial ecology.

H_2 emissions from senescing vegetation

For the first time, we report aboveground H_2 production from senescing vegetation, although the mechanism behind this flux is unknown. $F_{H2,A}$ emissions occurred during senescence, originated predominantly from deciduous-dominated portions of the landscape (Fig. 6), and were best predicted by maple sap flow. We propose that one or more of the following four processes that occur in or on woody or foliar tissues may be associated with the observed $F_{H2,A}$ emissions (discussed in more detail in Appendix S5): (i) abiotic photo-thermal production of H_2 from plant material may occur in the canopy biomass, even at natural insolation levels and temperatures as low as 25 °C (Derendorp *et al.*, 2011; Lee *et al.*, 2012); (ii) some plants release H_2 to cope with oxidative stress, such as caused by the overproduction of reactive oxygen species (Jin *et al.*, 2013), and may be an important mechanism during the physiological changes associated with plant senescence (Hu *et al.*, 2014); (iii) forests release volatile organic compounds during leaf senescence (Fall *et al.*, 2001) that can react with hydroxyl radical (OH) to form formaldehyde (HCHO); photodissociation of HCHO to H_2 could result in leaf emissions if occurring on surfaces or in liquid layers; and (iv) fermenting microorganisms in anaerobic environments such as sediments or rotting wood (e.g., Covey *et al.*, 2012) produce H_2 that may escape to the atmosphere together with CH_4, which is usually also produced in these environments, but may not scale up to be a significant source at Harvard Forest (Appendix S5). Future studies designed to measure H_2 fluxes in senescing vegetation by tower sampling, branch chambers, or in the laboratory are needed to evaluate these potential mechanisms. In addition, the ecological role of these aboveground H_2 emissions for plant-associated bacteria that scavenge atmospheric H_2 (e.g., Kanno *et al.*, 2016) would be a rich area for future work.

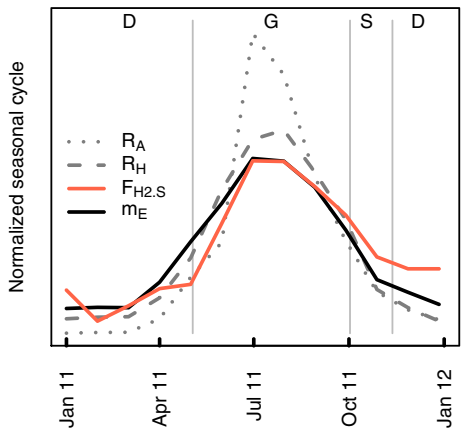

Fig. 7 H_2 soil uptake ($F_{H2,S}$), representing the H_2 energy supply to microbes, was more heavily weighted to the dormant (D) and senescent (S) season than soil respiration (R_S), which includes both heterotrophic (R_H) and autotrophic (R_A) respiration (measured in units of μmol m^{-2} s^{-1}) during the growing (G) season. Monthly mean seasonal cycles of R_A, R_H, $F_{H2,S}$, and the microbial maintenance energy demand (m_E; kJ day^{-1} C-mol^{-1} biomass) normalized to the area under seasonal cycle curves.

We observed bidirectional fluxes during senescence, during which soil uptake rates were offset by unexpected H_2 emissions from aboveground biomass. On a global basis, we estimate that aboveground emissions from senescing temperate mixed and deciduous forests, all forests, or all vegetated lands correspond, respectively, to 0.24, 2.3, or 6.2 Tg H_2 yr^{-1} by scaling the annual emissions observed at the Harvard Forest per unit area (Schmitt *et al.*, 2008). Thus, senescing vegetation as a H_2 source is likely only a minor component of the total atmospheric H_2 budget (<1% to 9% of total sources across studies reviewed in Ehhalt & Rohrer, 2009) on a similar magnitude as H_2 emissions from N_2 fixation. However, further study is needed to better constrain these H_2 emissions from senescing vegetation and their potential role in the atmospheric H_2 budget.

Concluding remarks

The measurements of H_2 ecosystem fluxes in a mixed deciduous forest contribute significantly to our

understanding of the seasonality and processes affecting atmospheric H_2. Our analysis shows that soil uptake is the key sink for atmospheric H_2 at Harvard Forest, and emissions of H_2 from the senescing forest canopy are an important, previously unrecognized source. Together, these processes drive bidirectional fluxes of H_2 that balance to a net annual ecosystem sink on an annual basis for atmospheric H_2 in mixed temperate stands at Harvard Forest. The importance of aboveground emissions of H_2 in other ecosystems is unknown, and future studies on H_2 emissions from senescing plant matter will be particularly valuable. The relationship between sap flow and H_2 soil and aboveground fluxes may be mechanistically related to transport processes within the tree or transpiration. As in our case, future studies will likely find it useful to consider H_2 cycling in the context of ecosystem phenology, which is now commonly characterized at many sites.

While this study spanned just over one year of measurements, from our attribution analysis, we anticipate that H_2 soil fluxes vary significantly with interannual variability in temperature (i.e., soil temperature, soil frost) and factors controlling the diffusion of H_2 into soil (i.e., water saturation and snow depth). These factors interact to create complex trade-offs, especially during the winter, between temperature and diffusion limitations, which are affected by the interplay between air temperature and the amount and type of precipitation (e.g., rain vs. snow). These interactions should be incorporated into model projections of the sensitivity of the H_2 sink to global change such as climate and land-use change to assess the impacts of these changes on the atmospheric H_2 burden and soil microorganisms utilizing atmospheric H_2.

Our results provide an *in situ* assessment of the role of H_2 energy metabolism by soil microorganisms by comparison with carbon metabolism. Recent advances in understanding the genetic and physiological basis for atmospheric H_2 scavenging microbes make it timely to investigate H_2 energy metabolism in other ecosystems and alongside genomic characterization, which was beyond the scope of this study. Comparative analyses of H_2 and CO_2 fluxes provide insights into the activity of H_2-consuming microbes in comparison with the broader microbial community, although these relationships are complex to tease apart. Future studies are needed to elucidate mechanisms underlying the relationship between H_2 uptake and respiration, such as the role of root exudates or rhizosphere community structure. Our H_2 data and the concurrent environmental measurements could be used to test or constrain ecosystem- and global-scale models of H_2 cycling, which have been traditionally data limited. At Harvard Forest, H_2 cycling was controlled by microorganisms and plants, making H_2 an exemplary system for the study of the biotic control of trace gas cycles.

Acknowledgements

We thank Kathleen Savage and Josh McLaren for help with respiration and snow data. LKM was supported by the following funding sources: NSF Graduate Research Fellowship, grants from NASA to MIT for the Advanced Global Atmospheric Gases Experiment (AGAGE), MIT Center for Global Change Science, MIT Joint Program on the Science and Policy of Global Change, MIT Martin Family Society of Fellows for Sustainability, MIT Ally of Nature Research Fund, MIT William Otis Crosby Lectureship, and MIT Warren Klein Fund, and NSF Postdoctoral Fellowship 1331214. Operation of the EMS flux tower was supported by the Office of Science (BER), U. S. Dept. of Energy (DE-SC0004985) and is a component of the Harvard Forest LTER supported by National Science Foundation. We acknowledge support for the PhenoCams at Harvard Forest from the National Science Foundation, through the Macrosystems Biology (EF-1065029) and LTER (DEB-1237491) programs. PHT was supported by a Charles Bullard Fellowship at Harvard University while writing this manuscript. We acknowledge support from the National Science Foundation (NSF DEB-1149929) and the Northeastern States Research Cooperative through funding by the USDA Forest Service to PT for measurements of sap flow. JT was partially supported by the U.S. Department of Energy Office of Biological and Environmental Research grant DE-SC0006951 and the National Science Foundation grants DBI-959333 and AGS-1005663.

References

Allen A (1995) Soil science and survey at Harvard Forest. *Soil Survey Horizons*, **36**, 133–142.

Barford CC, Wofsy SC, Goulden ML *et al*. (2001) Factors controlling long- and short-term sequestration of atmospheric CO_2 in a mid-latitude forest. *Science*, **294**, 1688–1691.

Boose E (2001) Fisher Meteorological Station at Harvard Forest since 2001. Harvard Forest Data Archive HF001. Available at: http://harvardforest.fas.harvard.edu:8080/exist/apps/datasets/showData.html?id=hf001 (accessed 26 August 2016).

Boose E (2009) Harvard Forest Snow Pillow since 2009. Harvard Forest Data Archive: HF155. Available at: http://harvardforest.fas.harvard.edu:8080/exist/apps/datasets/showData.html?id=hf155 (accessed 26 August 2016).

Bousquet P, Yver C, Pison I *et al*. (2011) A three-dimensional synthesis inversion of the molecular hydrogen cycle: sources and sinks budget and implications for the soil uptake. *Journal of Geophysical Research*, **116**, D01302.

Carslaw DC, Ropkins K (2012) openair - An R package for air quality data analysis. *Environmental Modelling and Software*, **27–28**, 52–61.

Commane R, Meredith LK, Baker IT *et al*. (2015) Seasonal fluxes of carbonyl sulfide in a mid-latitude forest. *Proceedings of the National Academy of Sciences*, **112**, 14162–14167.

Compton JE, Watrud LS, Porteous LA, DeGrood S (2004) Response of soil microbial biomass and community composition to chronic nitrogen additions at Harvard forest. *Forest Ecology and Management*, **196**, 143–158.

Conrad R (2006) Soil microbial communities and global climate change-methanotrophic and methanogenic communities as paradigms. In: *Modern Soil Microbiology*, 2nd edn (eds van Elsas JD, Trevors JT, Jansson JK), pp. 263–282. CRC Press, Vancouver.

Conrad R, Seiler W (1980) Contribution of hydrogen production by biological nitrogen fixation to the global hydrogen budget. *Journal of Geophysical Research*, **85**, 5493–5498.

Conrad R, Seiler W (1981) Decomposition of atmospheric hydrogen by soil microorganisms and soil enzymes. *Soil Biology and Biochemistry*, **13**, 43–49.

Constant P, Poissant L, Villemur R (2008a) Isolation of *Streptomyces* sp. PCB7, the first microorganism demonstrating high-affinity uptake of tropospheric H_2. *The ISME Journal*, **2**, 1066–1076.

Constant P, Poissant L, Villemur R (2008b) Annual hydrogen, carbon monoxide and carbon dioxide concentrations and surface to air exchanges in a rural area (Québec, Canada). *Atmospheric Environment*, **42**, 5090–5100.

Constant P, Poissant L, Villemur R (2009) Tropospheric H_2 budget and the response of its soil uptake under the changing environment. *Science of the Total Environment*, **407**, 1809–1823.

Constant P, Chowdhury SP, Pratscher J, Conrad R (2010) Streptomycetes contributing to atmospheric molecular hydrogen soil uptake are widespread and encode a putative high-affinity [NiFe]-hydrogenase. *Environmental Microbiology*, **12**, 821–829.

Constant P, Chowdhury SP, Hesse L, Conrad R (2011a) Co-localization of atmospheric H_2 oxidation activity and high affinity H_2-oxidizing bacteria in non-axenic soil and sterile soil amended with *Streptomyces* sp. PCB7. *Soil Biology and Biochemistry*, **43**, 1888–1893.

Constant P, Chowdhury SP, Hesse L, Pratscher J, Conrad R (2011b) Genome data mining and soil survey for the novel group 5 [NiFe]-hydrogenase to explore the diversity and ecological importance of presumptive high-affinity H_2-oxidizing bacteria. *Applied and Environmental Microbiology*, **77**, 6027–6035.

Covey KR, Wood SA, Warren RJ, Lee X, Bradford MA (2012) Elevated methane concentrations in trees of an upland forest. *Geophysical Research Letters*, **39**, L15705.

Derendorp L, Quist JB, Holzinger R, Röckmann T (2011) Emissions of H_2 and CO from leaf litter of *Sequoiadendron giganteum*, and their dependence on UV radiation and temperature. *Atmospheric Environment*, **45**, 7520–7524.

Derwent RG, Collins WJ, Johnson CE, Stevenson DS (2001) Transient behaviour of tropospheric ozone precursors in a global 3-D CTM and their indirect greenhouse effects. *Climatic Change*, **49**, 463–487.

Dong Z, Layzell DB (2001) H_2 oxidation, O_2 uptake and CO_2 fixation in hydrogen treated soils. *Plant and Soil*, **229**, 1–12.

Ehhalt DH, Rohrer F (2009) The tropospheric cycle of H_2: a critical review. *Tellus Series B*, **61**, 500–535.

Ehhalt DH, Rohrer F (2011) The dependence of soil H_2 uptake on temperature and moisture: a reanalysis of laboratory data. *Tellus Series B*, **63**, 1040–1051.

Ehhalt DH, Rohrer F (2013a) Deposition velocity of H_2: a new algorithm for its dependence on soil moisture and temperature. *Tellus Series B*, **65**, 19904.

Ehhalt D, Rohrer F (2013b) Dry deposition of molecular hydrogen in the presence of H_2 production. *Tellus Series B*, **65**, 20620.

Fall R, Karl T, Jordan A, Lindinger W (2001) Biogenic C5 VOCs: release from leaves after freeze-thaw wounding and occurrence in air at a high mountain observatory. *Atmospheric Environment*, **35**, 3905–3916.

Förstel H (1988) HT to HTO conversion in the soil and subsequent tritium pathway: field release data and laboratory experiments. *Fusion Science and Technology*, **14**, 1241–1246.

Förstel H, Führ F (1992) Trockene Deposition von Tritium in den Boden. *Forschungszentrum Jülich Annual Report*, pp. 45–51.

Gill AL, Gallinat AS, Sanders-DeMott R, Rigden AJ, Short Gianotti DJ, Mantooth JA, Templer PH (2015) Changes in autumn senescence in northern hemisphere deciduous trees: a meta-analysis of autumn phenology studies. *Annals of Botany*, **116**, 875–888.

Grant A, Witham CS, Simmonds PG, Manning AJ, O'Doherty S (2010) A 15 year record of high-frequency, *in situ* measurements of hydrogen at Mace Head, Ireland. *Atmospheric Chemistry and Physics*, **10**, 1203–1214.

Greening C, Berney M, Hards K, Cook GM, Conrad R (2014) A soil actinobacterium scavenges atmospheric H_2 using two membrane-associated, oxygen-dependent [NiFe] hydrogenases. *Proceedings of the National Academy of Sciences*, **111**, 4257–4261.

Greening C, Biswas A, Carere CR *et al.* (2015a) Genomic and metagenomic surveys of hydrogenase distribution indicate H_2 is a widely utilised energy source for microbial growth and survival. *The ISME Journal*, **10**, 761–777.

Greening C, Carere CR, Rushton-Green R *et al.* (2015b) Persistence of the dominant soil phylum Acidobacteria by trace gas scavenging. *Proceedings of the National Academy of Sciences*, **112**, 10497–10502.

Greening C, Constant P, Hards K *et al.* (2015c) Atmospheric hydrogen scavenging: from enzymes to ecosystems. *Applied and Environmental Microbiology*, **81**, 1190–1199.

Hayhoe K, Wake CP, Huntington TG *et al.* (2007) Past and future changes in climate and hydrological indicators in the US Northeast. *Climate Dynamics*, **28**, 381–407.

Hu H, Li P, Wang Y, Gu R (2014) Hydrogen-rich water delays postharvest ripening and senescence of kiwifruit. *Food Chemistry*, **156**, 100–109.

Hutchinson GL, Livingston GP, Healy RW, Striegl RG (2000) Chamber measurement of surface-atmosphere trace gas exchange: numerical evaluation of dependence on soil, interfacial layer, and source/sink properties. *Journal of Geophysical Research*, **105**, 8865–8875.

Jin Q, Zhu K, Cui W, Xie Y, Han B, Shen W (2013) Hydrogen gas acts as a novel bioactive molecule in enhancing plant tolerance to paraquat-induced oxidative stress via the modulation of heme oxygenase-1 signalling system. *Plant, Cell and Environment*, **36**, 956–969.

Kanno M, Constant P, Tamaki H, Kamagata Y (2016) Detection and isolation of plant-associated bacteria scavenging atmospheric molecular hydrogen. *Environmental Microbiology*, **18**, 2495–2506.

Khdhiri M, Hesse L, Popa ME *et al.* (2015) Soil carbon content and relative abundance of high affinity H_2-oxidizing bacteria predict atmospheric H_2 soil uptake activity better than soil microbial community composition. *Soil Biology and Biochemistry*, **85**, 1–9.

King GM (2003) Contributions of atmospheric CO and hydrogen uptake to microbial dynamics on recent Hawaiian volcanic deposits. *Applied and Environmental Microbiology*, **69**, 4067–4075.

Klosterman ST, Hufkens K, Gray JM *et al.* (2014) Evaluating remote sensing of deciduous forest phenology at multiple spatial scales using PhenoCam imagery. *Biogeosciences*, **11**, 4305–4320.

Lallo M, Aalto T, Laurila T, Hatakka J (2008) Seasonal variations in hydrogen deposition to boreal forest soil in southern Finland. *Geophysical Research Letters*, **35**, L04402.

Lallo M, Aalto T, Hatakka J, Laurila T (2009) Hydrogen soil deposition at an urban site in Finland. *Atmospheric Chemistry and Physics*, **9**, 8559–8571.

Langenfelds RL, Francey RJ, Pak BC, Steele LP, Lloyd J, Trudinger CM, Allison CE (2002) Interannual growth rate variations of atmospheric CO_2 and its $\delta^{13}C$, H_2, CH_4, and CO between 1992 and 1999 linked to biomass burning. *Global Biogeochemical Cycles*, **16**, 1048.

Le Texier H, Solomon S, Garcia RR (1988) The role of molecular hydrogen and methane oxidation in the water vapour budget of the stratosphere. *Quarterly Journal of the Royal Meteorological Society*, **114**, 281–295.

Lee H, Rahn T, Throop HL (2012) A novel source of atmospheric H_2: abiotic degradation of organic material. *Biogeosciences*, **9**, 4411–4419.

Maimaiti J, Zhang Y, Yang J, Cen YP, Layzell DB, Peoples M, Dong Z (2007) Isolation and characterization of hydrogen-oxidizing bacteria induced following exposure of soil to hydrogen gas and their impact on plant growth. *Environmental Microbiology*, **9**, 435–444.

Meredith LK (2016) Fluxes of molecular hydrogen (H_2) at the Harvard Forest EMS Tower in 2011. Harvard Forest Data Archive: HF288. Available at: http://harvardforest.fas.harvard.edu:8080/exist/apps/datasets/showData.html?id=hf288 (accessed 26 August 2016).

Meredith LK, Rao D, Bosak T *et al.* (2014a) Consumption of atmospheric hydrogen during the life cycle of soil-dwelling actinobacteria. *Environmental Microbiology Reports*, **6**, 226–238.

Meredith LK, Commane R, Munger JW, Dunn A, Tang J, Wofsy SC, Prinn RG (2014b) Ecosystem fluxes of hydrogen: a comparison of flux-gradient methods. *Atmospheric Measurement Techniques*, **7**, 2787–2805.

Morfopoulos C, Foster PN, Friedlingstein P, Bousquet P, Prentice IC (2012) A global model for the uptake of atmospheric hydrogen by soils. *Global Biogeochemical Cycles*, **26**, GB3013.

Munger JW, Wofsy SC (1999) Canopy-Atmosphere Exchange of Carbon, Water and Energy at Harvard Forest EMS Tower since 1991. Harvard Forest Data Archive: HF004. Available at: http://harvardforest.fas.harvard.edu:8080/exist/apps/datasets/showData.html?id=hf004 (accessed 26 August 2016).

Novelli PC, Lang PM, Masarie KA, Hurst DF, Myers R, Elkins JW (1999) Molecular hydrogen in the troposphere: global distribution and budget. *Journal of Geophysical Research*, **104**, 30427–30444.

O'Keefe J (2011) Phenology of woody species. Harvard Forest Data Archive. HF003. Available at: http://harvardforest.fas.harvard.edu:8080/exist/apps/datasets/showData.html?id=hf003 (accessed online 26 August 2016).

Osborne CA, Peoples MB, Janssen PH (2010) Detection of a reproducible, single-member shift in soil bacterial communities exposed to low levels of hydrogen. *Applied and Environmental Microbiology*, **76**, 1471–1479.

Philippot L, Raaijmakers JM, Lemanceau P, van der Putten WH (2013) Going back to the roots: the microbial ecology of the rhizosphere. *Nature Reviews Microbiology*, **11**, 789–799.

Piché-Choquette S, Tremblay J, Tringe SG, Constant P (2016) H_2-saturation of high affinity H_2-oxidizing bacteria alters the ecological niche of soil microorganisms unevenly among taxonomic groups. *PeerJ*, **4**, e1782.

Pieterse G, Krol MC, Batenburg AM *et al.* (2013) Reassessing the variability in atmospheric H_2 using the two-way nested TM5 model. *Journal of Geophysical Research: Atmospheres*, **118**, 3764–3780.

Richardson A (2008) PhenoCam Images and Canopy Phenology at Harvard Forest since 2008. Harvard Forest Data Archive: HF158. Available at: http://

harvardforest.fas.harvard.edu:8080/exist/apps/datasets/showData.html?id=hf158 (accessed 26 August 2016).

Richardson AD, Braswell BH, Hollinger DY, Jenkins JP, Ollinger SV (2009) Near-surface remote sensing of spatial and temporal variation in canopy phenology. *Ecological Applications*, **19**, 1417–1428.

Savage K, Davidson EA, Tang J (2013) Diel patterns of autotrophic and heterotrophic respiration among phenological stages. *Global Change Biology*, **19**, 1151–1159.

Schmitt CB, Belokurov A, Besançon C *et al*. (2008) In: *Global Ecological Forest Classification and Forest Protected Area Gap Analysis*. Analyses and recommendations in view of the 10% target for forest protection under the Convention on Biological Diversity (CBD). Freiburg: University of Freiburg.

Schmitt S, Hanselmann A, Wollschläger U, Hammer S, Levin I (2009) Investigation of parameters controlling the soil sink of atmospheric molecular hydrogen. *Tellus Series B*, **61**, 416–423.

Shoemaker JK, Keenan TF, Hollinger DY, Richardson AD (2014) Forest ecosystem changes from annual methane source to sink depending on late summer water balance. *Geophysical Research Letters*, **41**, 673–679.

Simmonds PG, Derwent RG, O'Doherty S *et al*. (2000) Continuous high-frequency observations of hydrogen at the Mace Head baseline atmospheric monitoring station over the 1994–1998 period. *Journal of Geophysical Research*, **105**, 12105–12121.

Smith-Downey NV, Randerson JT, Eiler JM (2006) Temperature and moisture dependence of soil H_2 uptake measured in the laboratory. *Geophysical Research Letters*, **33**, L14813.

Smith-Downey NV, Randerson JT, Eiler JM (2008) Molecular hydrogen uptake by soils in forest, desert, and marsh ecosystems in California. *Journal of Geophysical Research*, **113**, G03037.

Stein S, Selesi D, Schilling R, Pattis I, Schmid M, Hartmann A (2005) Microbial activity and bacterial composition of H_2-treated soils with net CO_2 fixation. *Soil Biology and Biochemistry*, **37**, 1938–1945.

Tjepkema J (1979) Nitrogen fixation in forests of central Massachusetts. *Canadian Journal of Botany*, **57**, 11–16.

Tromp TK, Shia R-L, Allen M, Eiler JM, Yung YL (2003) Potential environmental impact of a hydrogen economy on the stratosphere. *Science*, **300**, 1740–1742.

Urbanski S, Barford C, Wofsy S *et al*. (2007) Factors controlling CO_2 exchange on timescales from hourly to decadal at Harvard Forest. *Journal of Geophysical Research*, **112**, G02020.

Warwick NJ, Bekki S, Nisbet EG, Pyle JA (2004) Impact of a hydrogen economy on the stratosphere and troposphere studied in a 2-D model. *Geophysical Research Letters*, **31**, L05107.

Wofsy SC, Goulden ML, Munger JW *et al*. (1993) Net exchange of CO_2 in a mid-latitude forest. *Science*, **260**, 1314–1317.

Xiao X, Prinn RG, Simmonds PG *et al*. (2007) Optimal estimation of the soil uptake rate of molecular hydrogen from the advanced global atmospheric gases experiment and other measurements. *Journal of Geophysical Research*, **112**, D07303.

Yang X, Tang J, Mustard J (2014) Beyond leaf color: comparing camera-based phenological metrics with leaf biochemical, biophysical and spectral properties throughout the growing season of a temperate deciduous forest. *Journal of Geophysical Research: Biogeosciences*, **119**, 181–191.

Yashiro H, Sudo K, Yonemura S, Takigawa M (2011) The impact of soil uptake on the global distribution of molecular hydrogen: chemical transport model simulation. *Atmospheric Chemistry and Physics*, **11**, 6701–6719.

Yonemura S, Kawashima S, Tsuruta H (2000) Carbon monoxide, hydrogen, and methane uptake by soils in a temperate arable field and a forest. *Journal of Geophysical Research*, **105**, 14347–14362.

Yver CE, Pison IC, Fortems-Cheiney A *et al*. (2011a) A new estimation of the recent tropospheric molecular hydrogen budget using atmospheric observations and variational inversion. *Atmospheric Chemistry and Physics*, **11**, 3375–3392.

Yver C, Schmidt M, Bousquet P, Ramonet M (2011b) Measurements of molecular hydrogen and carbon monoxide on the Trainou tall tower. *Tellus Series B*, **63**, 52–63.

Supporting Information

Additional Supporting Information may be found in the online version of this article:

Figure S1 Heights of H_2 mole fraction measurements and relation to forest canopy.
Figure S2 Comparison of methods used to derive of soil and ecosystem H_2 fluxes.
Figure S3 Schematic of winter time webcam setup for monitoring snow depth.
Figure S4 Methods for deriving senescence information from PhenoCam.
Figure S5 Comparison of study period meteorology vs. 12-year climatology, part 1.
Figure S6 Comparison of study period meteorology vs. 12-year climatology, part 2.
Figure S7 Results from artificial neural network analysis of H_2 net ecosystem exchange.
Figure S8 Quantile plots of the relationship between $FH_{2,A}$ and environmental variables.
Table S1 H_2 and CO_2 soil fluxes and microbial maintenance energy demand across phenological seasons.
Appendix S1 Supplementary materials and methods.
Appendix S2 12-year recent climatology (2001–2012) at Harvard Forest.
Appendix S3 Environmental drivers of H_2 fluxes.
Appendix S4 Calculations of energy derived by microbes from H_2 and carbon substrates.
Appendix S5 Detailed potential mechanisms for H_2 emissions from senescing vegetation.